

Supplemental Data

Fig. S1. **Double reciprocal plot of the effect of acetyl-CoA concentration on hNaa50p NAT activity at different peptide concentrations.** The $^1\text{MLGP-RRR}^{24}$ concentrations were (\circ) 37 μM , (\bullet) 75 μM , (\square) 150 μM , or (\blacksquare) 300 μM .

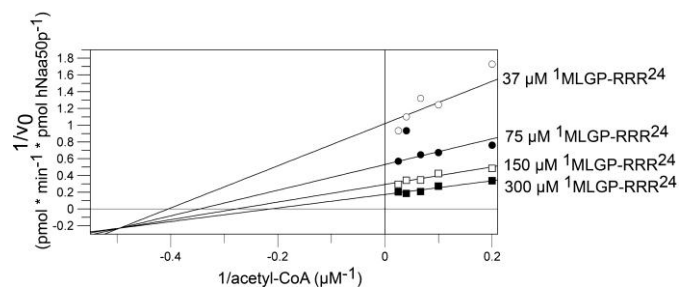
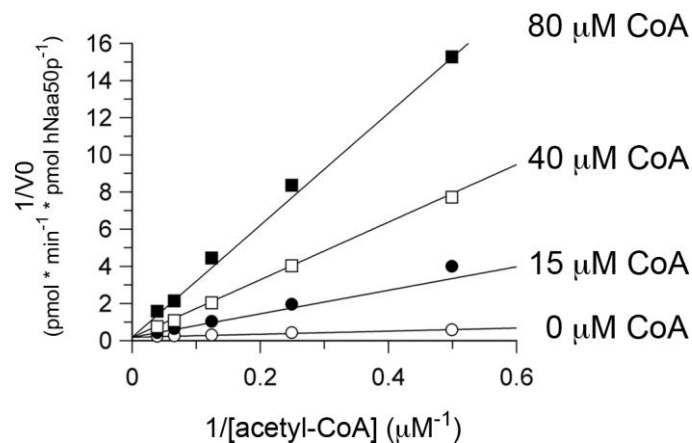


Fig. S2. Double reciprocal plot of effect of acetyl-CoA concentration on hNaa50p NAT activity in the presence of the reaction product CoA and the dead-end analogue desulfo-CoA. **A.** The reactions were conducted in 50 mM Tris-HCl (pH 8.5), 50 nM purified GST-hNaa50p and $1 \times K_m$ (80 μM) of $^1\text{MLGP-RRR}^{24}$. The acetyl-CoA concentration varied from 2 to 25 μM . The CoA concentrations were: (\circ) 0 μM , (\bullet) 15 μM , (\square) 40 μM , or (\blacksquare) 80 μM . **B.** The reactions were performed as described for A, except CoA was replaced with desulfo-CoA at: (\circ) 0 μM , (\bullet) 10 μM , (\square) 20 μM , or (\blacksquare) 60 μM .

A



B

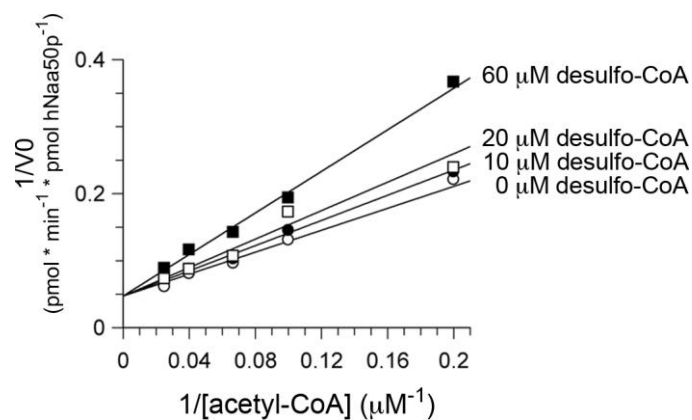


Fig. S3. **Double reciprocal plot of effect of peptide substrate concentration on hNaa50p NAT activity in the presence of the reaction product CoA.** Reactions were conducted in 50 mM Tris-HCl (pH 8.5) with 30 nM purified GST-hNaa50p and 100 μ M acetyl-CoA. The 1 MLGP-RRR 24 concentrations varied from 30 to 500 μ M. CoA concentrations were: (\circ) 0 μ M, (\bullet) 15 μ M, (\square) 40 μ M, or (\blacksquare) 80 μ M.

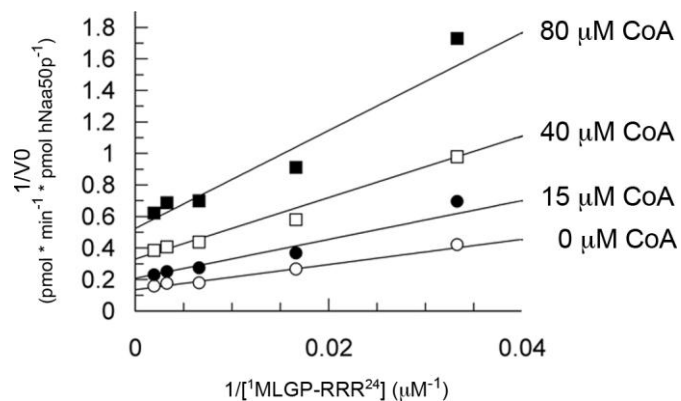


Fig. S4A. **Product inhibition using acetylated peptide against peptide substrate.** No significant inhibition was observed using acetylated peptides as product inhibitors, against $^1\text{MLGP-RRR}^{24}$. The concentration of fixed substrate (acetyl-CoA) was at approximately $1xK_m = 10 \mu\text{M}$.

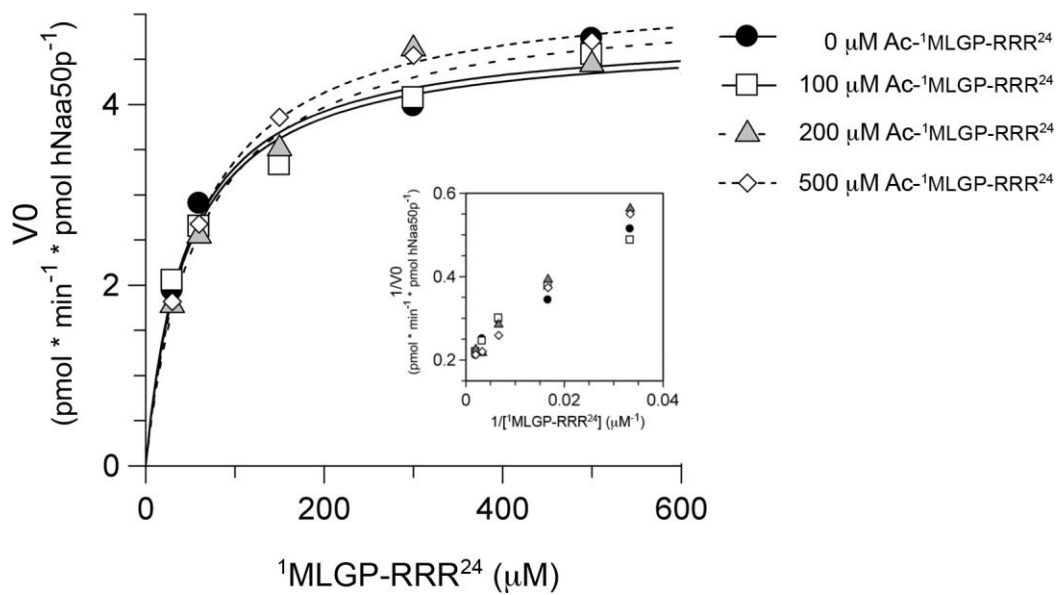
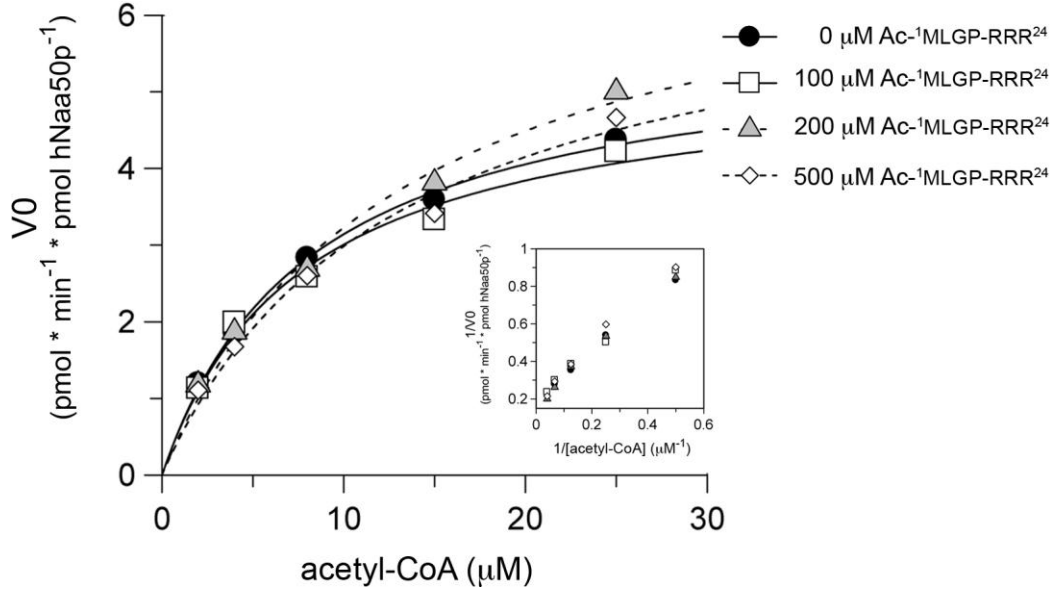


Fig. S4B. **Product inhibition using acetylated peptide against acetyl-CoA as variable substrate.** No significant inhibition was observed using acetylated peptides as product inhibitors against the substrate acetyl-CoA. The concentration of fixed substrate ($^1\text{MLGP-RRR}^{24}$) was at approximately $1 \times K_m = 80 \mu\text{M}$.



For two substrate double reciprocal plots, initial rates were fit by a nonlinear approach to either, Eq 1 (parallel line pattern),

$$v = \frac{V_{\text{MAX}} \times [\text{acCoA}] \times [^1\text{MLGP-RRR}^{24}]}{K_b \times [\text{acCoA}] + K_a \times [^1\text{MLGP-RRR}^{24}] + [\text{acCoA}] \times [^1\text{MLGP-RRR}^{24}]},$$

where K_a is the K_m of acetyl-CoA, and K_b is the K_m of $^1\text{MLGP-RRR}^{24}$, or

Eq2:

$$v = \frac{V_{\text{MAX}} \times [\text{acCoA}] \times [^1\text{MLGP-RRR}^{24}]}{\alpha K_a \times K_b + K_b \times [\text{acCoA}] + K_a \times [^1\text{MLGP-RRR}^{24}] + [\text{acCoA}] \times [^1\text{MLGP-RRR}^{24}]},$$

where K_a is the K_m of acetyl-CoA, and K_b is the K_m of $^1\text{MLGP-RRR}^{24}$, α is the interaction factor for the peptide binding to the enzyme-acetyl-CoA complex.

For competitive inhibition, the initial velocity data were fit to

Eq 3:

$$v = \frac{V_{\text{MAX}} \times [S]}{K_m \left(1 + \frac{[I]}{K_i} \right) + [S]}, \text{ where } K_i \text{ is the inhibitor constant and } V_{\text{MAX}} \text{ is the apparent maximal velocity.}$$

For non-competitive inhibition, initial velocity data were fit to

Eq 4:

$$v = \frac{V_{\text{MAX}} \times [\text{S}] \times \left(\frac{1}{1 + \frac{[\text{I}]}{K_i}} \right)}{K_m + [\text{S}]}, \quad V_{\text{MAX}} \text{ is the apparent maximal velocity.}$$

All of the above fits of the data were made using the GraFit ver. 7 software package.

Fig. S5. **The secondary structure composition of hNaa50p in complex with acetyl-CoA determined using the chemical shift index (CSI).** C^α (brown) and C' (light green) chemical shift deviations in ppm compared to their random coil values are plotted against the amino acid sequence numbers. The values between the horizontal lines indicate random coil values. More than three consecutive amino acids with a shift deviation above 0.7 ppm (C^α) and 0.5 ppm (C') respectively are most likely situated in an α -helix, whereas more than three consecutive amino acids with a shift deviation below these values are most likely positioned in β -strands. According to this simple approximation, hNaa50p contains four helices (indicated by boxes) at the following sequence positions: 17-26 (this helix might already start at His14), 33-38, 87-104 and 118-126. In addition, hNaa50p is characterized by some long range β -strands (indicated by arrows). The strands are situated at the following positions: 5-9 (probably extended to Thr12), three consecutive strands interrupted with turns at 46-74, 108-111, and three consecutive strands interrupted with turns at 129-156. The secondary structures derived from solution NMR are overall in good agreement with the positions of the secondary structures observed in the hNaa50p-acetyl-CoA complex in a single crystal (PDB ID 2OB0). Note that the second to last strand might be an artefact caused by reduced flexibility in the structure in that particular region.

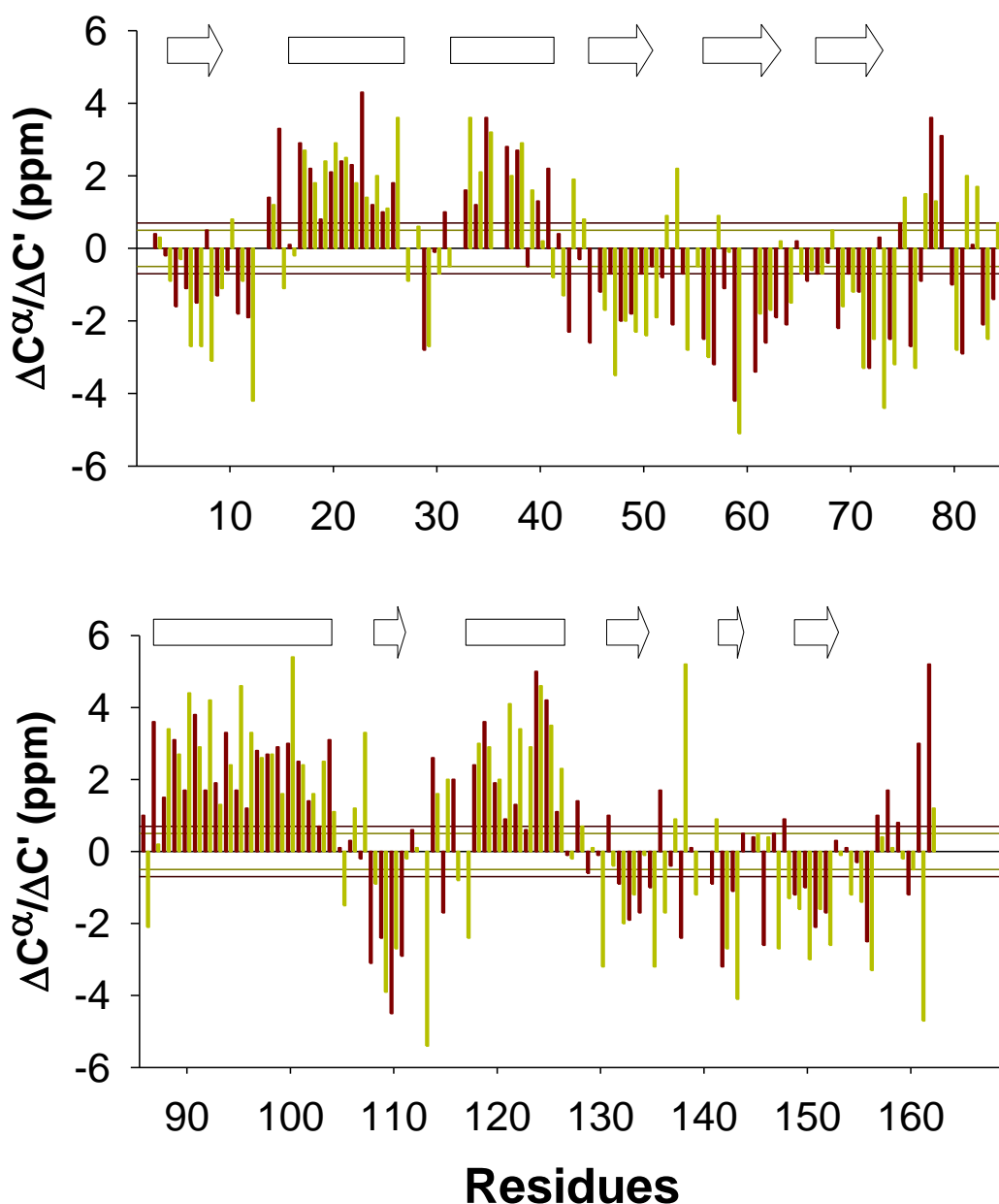
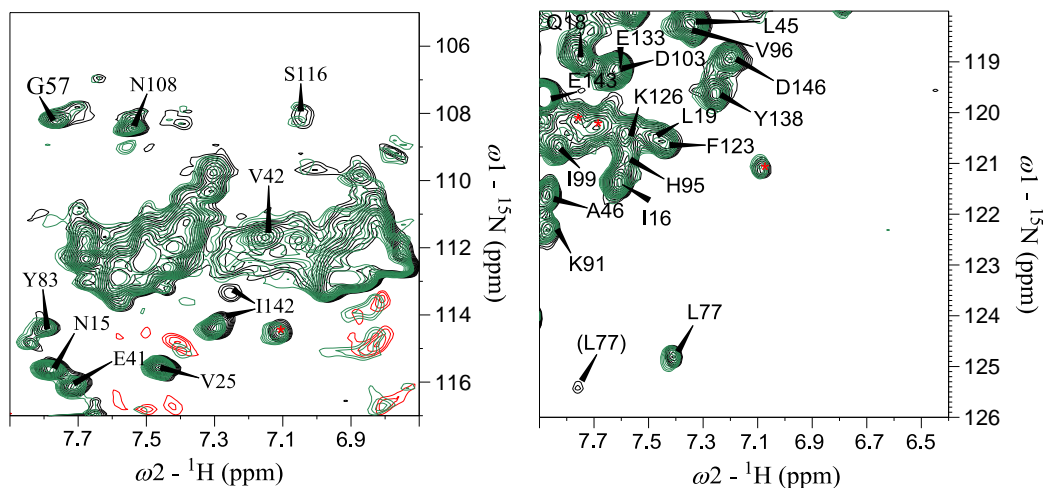


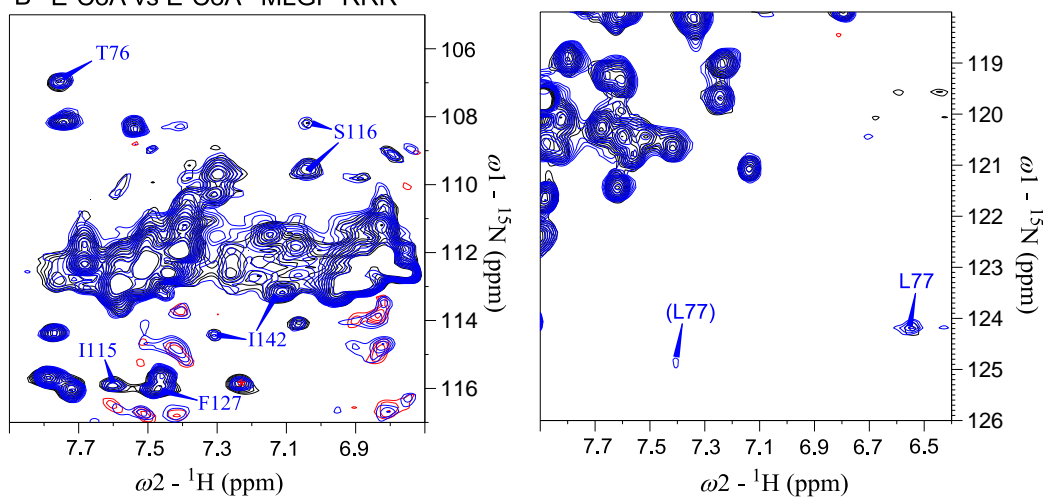
Fig. S6.

A. Overlay of two expanded regions of the 2D ^1H - ^{15}N HMQC spectrum of hNaa50p (black) and hNaa50p with peptide (green). **B.** Overlay of the HMQC spectra of hNaa50p with CoA (black) and hNaa50p with CoA and peptide (blue). **C.** Overlay of the HMQC spectra of hNaa50p with CoA (black) and hNaa50p with CoA and acetylated peptide (blue). Only peaks that show significant chemical shift changes upon binding are assigned in panels **B** and **C**. Peaks with unknown identity are indicated with a red asterisk.

A E vs E- $^1\text{MLGP-RRR}^{24}$



B E-CoA vs E-CoA- $^1\text{MLGP-RRR}^{24}$



C E-CoA vs E-CoA-Ac $^1\text{MLGP-RRR}^{24}$

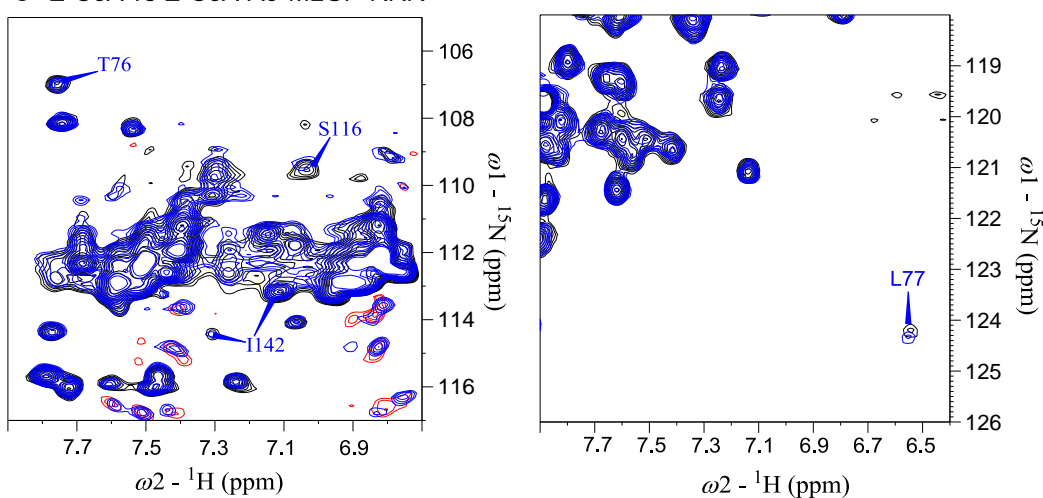


Fig. S7.

A. Overlay of two expanded regions of the 2D ^1H - ^{15}N HMQC spectra of hNaa50p with CoA and acetylated peptide (black) and hNaa50p with CoA and peptide (blue) at 310 K. The peaks of the former spectrum coincide with those of the hNaa50p-CoA complex. The second peak for Tyr73 that is observed for hNaa50p in complex with CoA and $^1\text{MLGP-RRR}^{24}$ coincides with the peak in the spectrum of the hNaa50p-acetyl-CoA complex. **B.** Overlay of two expanded regions of the 2D ^1H - ^{15}N HMQC spectra of the hNaa50p H112A mutant with acetyl-CoA (black) and the mutant in the presence of both acetyl-CoA and peptide (blue) at 298 K. The chemical shifts of Tyr110 and Lys135 change slightly in the presence of both substrates, whereas the position and intensities of two of the three peaks of Tyr73 differ between the two spectra.

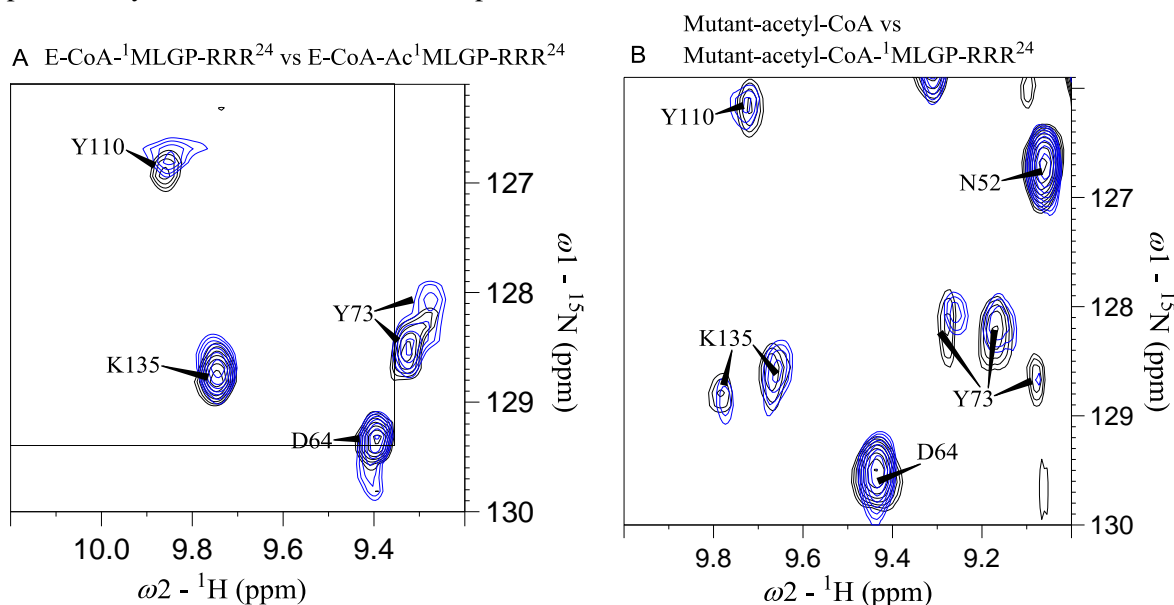


Fig. S8.

A. Expanded region of the 2D ^1H - ^{15}N HMQC spectrum of hNaa50p (black) and hNaa50p with acetyl-CoA (blue) containing Tyr124. **B.** Positioning of Tyr124 and Leu77 to each other and to acetyl-CoA (blue) in the crystal structure of the hNaa50p-acetyl-CoA complex. The structure was created with the PyMOL Molecular Graphics System, Version 1.3, Schrödinger, LLC.

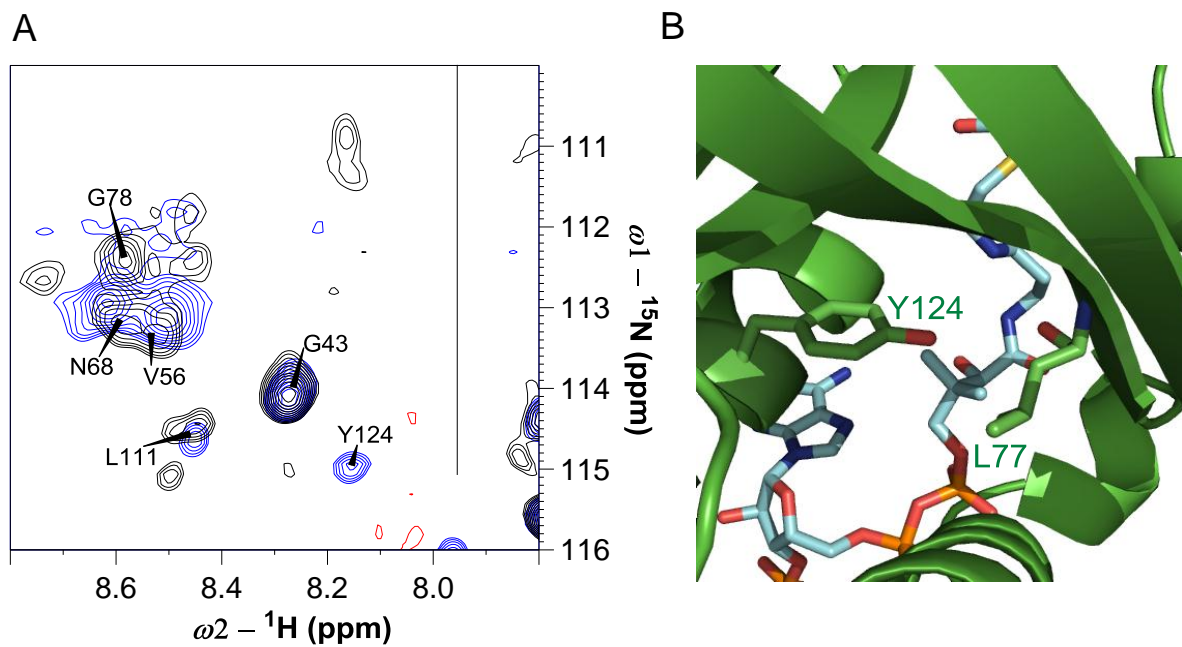


Fig. S9.

Amino acids involved in the substrate binding (PDB ID 2OB0). Leu77, the residue that is most affected by the addition of acetyl-CoA (blue), is closest to the cysteamine moiety, whereas Val29 and Ile142 change chemical shifts most likely as an effect of an “induced fit” response. Tyr73 and His112 are supposedly involved in the catalytic activity and are part of the hydrophobic pocket that binds to the peptide substrate. The figure was created with the PyMOL Molecular Graphics System, Version 1.3, Schrödinger, LLC.

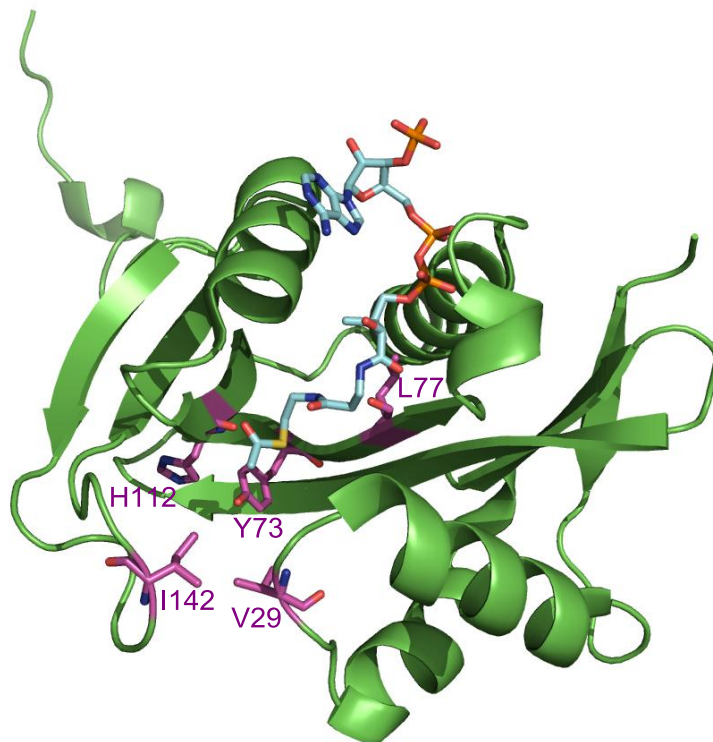


Table S1: Acquisition parameters of NMR-experiments

Experiment	Acquisition		Resonances			Complex points			Carrier ν (ppm)			Spectral width (ppm)		
	time (hrs)	Scans	X	Y	Z	X	Y	Z	X	Y	Z	X	Y	Z
HNCO	8	4	H ^N	N ^H	C ^α	2048	32	48	4.68	118.0	174.0	16.3	32.1	80.0
HN(CA)CO	12	4	H ^N	N ^H	C ^α	2048	48	45	4.68	118.0	174.0	16.3	32.1	80.0
HNCA	20	8	H ^N	N ^H	C ^α	2048	32	60	4.68	118.0	56.0	16.3	32.1	30.0
HN(CO)CA	20	8	H ^N	N ^H	C ^α	2048	32	60	4.68	118.0	56.0	16.3	32.1	30.0
CBCA(CO)NH	48	8	H ^N	N ^H	C ^α /C ^β	2048	47	96	4.68	118.0	46.0	16.3	32.1	18.7
HNCACB	48	8	H ^N	N ^H	C ^α /C ^β	2048	47	96	4.68	118.0	46.0	16.3	32.1	18.7
CC(CO)NH	81	32	H ^N	N ^H	C ^{ali}	2048	32	144	4.68	117.0	36.2	12.0	30.0	70.0
¹ H- ¹⁵ N HSQC	1	32	H ^N	N ^H		2048	128		4.68	117.0		12.0	30.0	
¹ H- ¹⁵ N HMQC	0.3	64	H ^N	N ^H		700	128		4.68	117.0		12.0	30.0	
MUSIC [†] :														
A <i>i</i> +1	9	288	H ^N	N ^H		2048	64		4.68	117.0		12.0	30.0	
S <i>i</i> +1	2	96	H ^N	N ^H		2048	48		4.68	117.0		12.0	30.0	
DNG <i>i</i> +1	6	192	H ^N	N ^H		2048	64		4.68	117.0		12.0	30.0	
EQG <i>i</i> +1	5	160	H ^N	N ^H		2048	64		4.68	117.0		12.0	30.0	
EQG <i>i,i</i> +1	10	320	H ^N	N ^H		2048	64		4.68	117.0		12.0	30.0	
VIA <i>i</i> +1	22	720	H ^N	N ^H		2048	64		4.68	117.0		12.0	30.0	
VIA <i>i,i</i> +1	23	768	H ^N	N ^H		2048	64		4.68	117.0		12.0	30.0	

[†] Interpretation of the acronyms of the amino acid edited pulse programmes (MUSIC): *i*+1 defines the succeeding residue to a certain type of amino acid, e.g. A *i*+1 yields a 2D ¹H-¹⁵N HSQC spectrum containing only residues following alanine, while *i,i*+1 results in spectra containing both signals of the selected amino acid(s) and, very weakly, of their successors.

Table S2: ^{13}C , ^{15}N and ^1H resonance assignments for hNaa50p with acetyl-CoA at pH 7.4 and 310 K.

Residue	N^{H}	H^{N}	C'	C^{α}	C^{β}	Others
M1						
K2						
G3			174.1	45.2		
S4	116.2	8.09	173.4	57.5	64.0	
R5	123.4	8.18	175.0	55.9	31.0	C^{γ} 27.6, C^{δ} 43.1
I6	125.0	8.34	175.6	60.1	39.2	C^{δ} 18.0
E7	125.9	8.75	174.4	54.2	34.2	C^{γ} 35.8
L8	120.7	8.84	177.4	52.8	42.3	C^{δ} 26.9, 26.3
G9	109.3	9.58	172.2	44.0		
D10	119.8	8.42	176.4	54.9	41.1	
V11	123.2	9.15	175.2	62.2	31.5	C^{γ} 22.4, 21.6
T12	120.2	9.67	173.4	58.8	69.7	C^{γ} 21.1
P13						
H14			176.6	56.9	30.6	
N15	115.5	7.79	178.3	52.6	38.7	
I16	121.2	7.62	176.6	63.0	37.7	C^{γ} 17.7, C^{δ} 15.0
K17	120.6	8.36	179.2	59.6	31.7	C^{γ} 24.5, C^{ϵ} 41.6
Q18	118.8	7.74	178.2	58.3	28.1	
L19	120.5	7.42	177.5	58.5	41.5	C^{γ} 27.0, C^{δ} 21.4, 20.3
K20	117.9	8.06	178.4	59.8	32.1	C^{ϵ} 41.2
R21	117.9	7.56	178.7	59.0	29.8	C^{δ} 43.1
L22	118.7	8.01	178.9	58.0	41.9	C^{γ} 30.0, C^{δ} 27.0, 25.7
N23	117.9	8.63	179.0	55.4	36.6	
Q24	118.7	8.21	177.3	58.4	28.4	
V25	115.5	7.47	177.9	64.3	32.5	C^{γ} 21.8
I26	118.5	8.06	178.9	66.0	39.6	
F27	117.6	8.43		57.0	40.1	
P28			176.0	63.5	30.9	
V29	116.5	6.96	174.3	60.3	33.6	C^{γ} 22.8, 20.0
S30			173.7	57.5	63.6	
Y31	124.5	8.09	176.8	58.0		
N32						
D33			178.8	57.7	40.4	
K34	120.9	8.12	177.4	59.1	32.2	C^{ϵ} 42.2
F35	119.9	7.78	179.3	61.2	38.6	
Y36						
K37			179.1	58.8	32.3	
D38	120.4	8.37	179.9	57.0	39.5	
V39	117.5	7.70	176.4	64.8	31.8	C^{γ} 22.4, 21.4
L40	117.4	7.11	178.1	56.2	41.4	C^{δ} 25.8
E41	115.9	7.71	177.9	56.3	30.5	C^{γ} 35.8
V42	111.6	7.16	177.3	61.9	31.7	C^{γ} 20.5, 19.3
G43	113.9	8.28	175.7	47.1		
E44	122.1	8.84	175.3	58.0	29.7	C^{γ} 35.7
L45	118.2	7.32	174.2	56.0	40.8	C^{γ} 28.1, C^{δ} 25.5, 23.5
A46	121.5	7.89	175.9	50.8	22.0	
K47	117.2	8.84	175.7	53.3	37.1	
L48	119.7	8.58	174.7	54.1	45.3	C^{γ} 25.4
A49	122.6	8.32	175.2	50.3	21.3	
Y50	120.9	9.30	174.6	56.6	41.8	
F51	123.0	9.05	175.3	56.0	42.5	
N52	126.4	9.03	174.2	54.6	36.5	
D53	109.2	8.96	174.8	56.6	39.7	
I54	122.0	8.07	175.7	60.1	46.2	C^{γ} 26.6
A55	130.5	8.76	176.9	52.2	17.3	
V56	113.3	8.48	174.4	60.2	34.9	C^{γ} 19.9, 18.7
G57	108.0	7.75	170.2	46.1		
A58	119.0	8.58	175.7	52.7	23.7	
V59	119.0	8.85	172.8	58.0	33.6	
C60						
C61			171.4	56.5	31.8	
R62	116.2	9.07	173.7	54.8	34.3	C^{δ} 43.7
V63	123.3	8.87	175.0	63.4	31.8	C^{γ} 21.6
D64	129.4	9.42	174.7	53.0	43.8	
H65	125.0	8.75	175.1	55.3	30.3	

Table S2: continued

Residue	N ^H	H ^N	C ^γ	C ^α	C ^β	Others
S66	117.8	8.23	174.4	57.7	64.4	
Q67	122.1	8.12	175.3	56.4	26.9	
N68	112.9	8.57	174.4	54.4	37.8	
Q69	117.5	7.75	174.1	54.6	32.7	C ^γ 33.8
K70	125.2	9.40	175.0	56.3	33.3	
R71	125.6	8.99	174.5	53.8	34.9	C ^δ 43.8
L72	125.7	8.88	173.8	53.2	41.8	C ^γ 27.3, C ^δ 25.8, 24.5
Y73	128.1	9.28	175.8	54.4	39.8	
I74	127.9	8.08	172.6	61.2	37.4	C ^γ 21.8, 18.0, C ^δ 13.7
M75	122.9	9.02	176.6	57.9	33.6	
T76	106.5	7.70	172.4	59.9	70.6	C ^γ 16.9
L77	124.2	6.86	176.0	57.4	42.8	
G78	112.5	8.60	170.1	46.6		
C79	116.1	8.95		55.5	31.5	
L80	125.2	8.88	176.1	52.9	44.0	
A81	119.8	9.23	174.2	54.5	17.3	
P82			176.1	64.6	30.5	C ^δ 50.4
Y83	114.6	7.84	173.1	56.6	37.9	
R84	117.8	6.67	175.1	57.0	31.4	
R85	117.0	9.52	176.2	57.3		
L86			178.1	53.6	43.7	C ^δ 26.3, 25.5
G87	111.6	9.57	177.2	45.2		
I88	125.5	9.35	178.0	66.4	35.8	C ^γ 29.0
G89	112.6	9.69	176.6	47.8		
T90	121.0	9.45	175.5	68.9		C ^γ 21.0
K91	122.5	7.86	180.2	59.7	31.9	C ^ε 41.8
M92	117.7	8.27	177.2	61.1	34.4	
L93	120.7	8.99	178.8	57.2	40.7	C ^δ 25.6, 22.6
N94	117.8	9.08	178.2	56.2	37.6	
H95	120.5	7.65	176.7	60.5	30.3	
V96	118.1	7.40	178.0	66.6	31.4	C ^γ 22.5
L97	119.4	8.73	179.7	58.5	40.1	C ^δ 26.0
N98	119.1	8.34	177.7	56.4	38.4	
I99	120.5	7.83	179.5	64.5	38.1	C ^γ 27.7, C ^δ 16.6
C100	117.4	7.73	177.7	63.8	26.7	
E101	122.9	8.54	178.4	59.3	29.3	C ^γ 35.8
K102	117.7	8.01	177.8	58.4	32.1	C ^γ 24.7, C ^ε 41.6
D103	119.0	7.66	177.7	56.8	43.2	
G104	102.8	8.17	176.4	46.4		
T105	111.1	9.04	175.0	61.9	69.5	C ^γ 21.0
F106	120.2	8.30	176.0	59.2	40.0	
D107	119.9	9.67	177.0	57.4	43.4	
N108	108.3	7.55	171.8	52.9	41.1	
I109	118.0	8.27	174.4	58.8	45.9	
Y110	126.4	9.75	171.2	55.9	42.0	
L111	114.6	8.50	174.1	55.6	43.2	C ^δ 26.0
H112			175.6	56.0	33.8	
V113*	127.8	7.86		57.6		
Q114			179.2	57.5	30.0	
I115	116.4	7.65	175.0	64.8		C ^δ 16.3
S116*	109.6	7.06	175.6	57.4	63.3	
N117	123.7	8.02	175.0	51.3	36.4	
E118	124.0	8.10	178.4	59.8	29.8	
S119	113.4	8.79	177.2	61.3	62.4	
A120	122.7	7.39	178.7	54.8	19.9	
I121	118.9	8.10	177.5	67.0	38.1	C ^γ 25.7, 22.9, C ^δ 14.3
D122	118.2	8.33	178.2	57.8	40.8	
F123	119.6	7.46	176.2	61.0	38.7	
Y124	114.7	8.23	180.5	63.4	36.9	
R125	121.9	8.79	180.5	60.0	29.7	C ^γ 27.8, C ^δ 43.5
K126	119.9	7.42	177.6	59.0	31.3	C ^ε 41.5
F127	116.1	7.56	175.7	57.7	39.6	
G128	106.7	8.05	174.8	45.9		
F129	118.1	7.67	175.1	58.1	39.9	
E130	119.2	8.54	175.7	53.8	33.3	C ^γ 35.8

TableS2: continued

Residue	N ^H	H ^N	C ^γ	C ^α	C ^β	Others
I131	123.0	8.97	177.5	62.6	38.0	C ^γ 27.6, C ^δ 17.5
I132	123.5	8.80	175.6	61.0	39.4	C ^γ 26.5, C ^δ 18.2
E133	119.0	7.62	174.0	55.7	32.8	
T134	120.4	8.85	173.6	62.9	70.7	C ^γ 21.3
K135	128.5	9.76	175.3	53.7	33.0	C ^ε 41.3
K136	125.4	8.71	178.1	55.1	31.8	C ^δ 24.3, C ^ε 41.3
N137	118.8	9.53	174.7	54.5	36.8	
Y138	119.5	7.26	176.6	61.0	40.4	
Y139	117.1	8.81	175.8	57.4	39.9	
K140						
R141			175.4	57.4	29.7	C ^δ 42.9
I142	113.6	7.23	173.5	60.1	40.7	C ^γ 25.7, C ^δ 17.8
E143	119.4	7.98	175.0	52.6	32.4	
P144			176.5	62.9		
A145	123.2	8.90	177.6	52.9	20.6	
D146	118.8	7.22	174.6	54.5	41.7	
A147	121.5	8.68	177.4	50.0	23.9	
H148	119.4	9.13	175.7	54.8	33.3	
V149	121.3	8.88	175.8	61.5	32.0	C ^γ 20.9
L150	128.1	8.79	176.1	52.7	43.8	
Q151			174.3	54.5	34.0	
K152	130.6	9.08	174.8	54.1	34.0	
N153	127.1	8.91	175.2	53.7	38.6	
L154	123.2	8.08	176.9	54.8	42.0	C ^γ 27.2, C ^δ 21.9, 20.8
K155	120.2	8.06	176.0	55.5	33.0	C ^γ 24.0, C ^ε 42.0
V156	122.3	8.05	174.6	59.7	32.1	
P157 [‡]			176.9	63.4	32.2	C ^δ 50.9
S158	116.4	8.40	175.3	58.5	63.9	
G159	111.0	8.45	173.9	45.4		
Q160	119.9	8.17	174.9	55.7	29.5	C ^γ 33.9
N161	125.4	8.05	173.9	53.3	39.9	
A162	129.6	7.83	182.4	53.6	19.8	
D163						
V164						
Q165						
K166						
T167						
D168						
N169						

* Ambiguous assignment.

[‡] P157 is present in both cis- and trans-conformation, thus all following amino acids have two NH-peaks. Only the stronger trans-peaks are shown in the table.